MAHMOOD M. SALEH
ORCID: 0009-0006-6128-8273
Department of Physics, Faculty of Sciences, University of Sfax, Tunisia
E-mail: mms.82.2006@gmail.com

HAMADI KHEMAKHEM
ORCID: 0000-0002-1753-8451
Department of Physics, Faculty of Sciences, University of Sfax, Tunisia
E-mail: hamadi.khemakhem@fss.usf

ISHMAEL K. JASSIM
ORCID: 0009-0002-2997-6819
Department of Physics, College Education of Pure Science, Tikrit University, Iraq
E-mail: prof.i.k.jassim@gmail.com

RAED HASHIM AL-SAQA
ORCID: 0000-0003-3538-457X
Directorate General of Education, Nineveh, Iraq
E-mail: raed.h.alsaqa@st.edu.tu.iq

DOI: 10.15199/40.2024.1.2

Structure and mechanical properties of cermet Ni-Al/MSZ thick coating prepared by flame spraying technique

Struktura i właściwości mechaniczne grubowarstwowej powłoki cermetalowej Ni-Al/MSZ przygotowanej techniką natrysku płomieniowego

The aim of this study was to obtain a thick protective cermet coating on API 5L (carbon steel) pipes, used in the oil industry. A new method involving flame spray coating has been selected to produce thick ceramic-metal coatings of Ni-Al/MgO-ZrO_2 under optimal spraying parameters. Structural properties were measured by X-ray diffraction (XRD). Morphology was determined by means of scanning electron microscopy (SEM). The elemental composition in the cermet coating was confirmed by energy dispersive spectroscopy (EDS). Deposition efficiency was found to be an important factor as demonstrated by adhesion force results obtained using the pull-out tensile test. The results show that the best spray distance is 20 cm, as it ensures good interaction between the layers, a high adhesion force value of 8.4 MPa, a uniform microstructure, low porosity, a hardness of 166.4 HV, and a coating thickness of approximately 1.85 mm. X-ray results clearly show that the cermet coating consists of numerous phases, such as tetragonal (T), monoclinic, and face center cubic (FCC). SEM images revealed that the typical particle-containing microstructures consisted of spherical shapes with elongated agglomerations. Finally, based on the results obtained, it can be concluded that flame spray coating provides a significant improvement in performance.

Keywords: cermet coating, flame spraying, MgO-ZrO_2, carbon steel, self-bonding Ni-Al

Celem pracy było uzyskanie grubej ochronnej powłoki cermetalowej na rurach API 5L (ze stali węglowej), stosowanych w przemyśle naftowym. Wybrano nową metodę natryskiwania płomieniowego w celu wytworzenia grubych powłok ceramiczno-metalowych Ni-Al/MgO-ZrO_2 przy optymalnych parametrach natryskiwania. Właściwości strukturalne zostały zmierzone za pomocą dyfrakcji rentgenowskiej (XRD). Morfologię określono za pomocą skaningowej mikroskopii elektronowej (SEM). Skład pierwiastkowy powłoki cermetalowej ustalono, używając spektroskopii dyspersji energii (EDS). Stwierdzono, że wydajność osadzania jest ważnym czynnikiem, o czym świadczą wyniki pomiaru siły adhezji uzyskane w próbie rozciągania. Z badań wynika, że najlepsza odległość natryskiwania wynosi 20 cm – zapewniona jest wówczas dobra interakcja między warstwami, wysoka wartość siły adhezji: 8,4 MPa, jednolita mikrostruktura, niska porowatość, twardość wynosi 166,4 HV, a grubość powłoki ok. 1,85 mm. Badania rentgenowskie pozwoliły ustalić, że powłoka cermetalowa składa się z wielu faz: tetragonalnej (T), jednoskośnej i FCC. Obrazy SEM ujawniły, że typowe mikrostruktury zawierające cząstki składały się z kulistych struktur tworzących wydłużone aglomeracje. Na podstawie uzyskanych wyników można stwierdzić, że zastosowana metoda natryskiwania płomieniowego zapewnia znaczną poprawę właściwości ochronnych.

Słowa kluczowe: powłoka cermetalowa, natryskiwanie płomieniowe, MgO-ZrO_2, stal węglowa, samospiekający się Ni-Al

Received / Otrzymano: 31.07.2023. Accepted / Przyjęto: 2.10.2023

1. Introduction

The main engineering concern in the use of assets is their surface, which is often subject to wear and corrosion [1]. Corrosion is a significant economic problem [2] and is responsible for the loss of over 30% of industrial parts, oil pipelines, structures and generated energy. Petroleum products such as carbon steel tanks, pipes and pumps are particularly susceptible to corrosion due to the presence of water, which can contain gases including H_2S and CO_2, as well as salts [3]. Thermal spray coatings are a new method used today for wear and corrosion protection [4]. The flame coating obtained acts as a barrier protecting structures such as oil tanks, valves and oil pipes [5]. Coatings of magnesia-stabilised zirconia (MgO-ZrO_2) powders have low thermal conductivity and a high melting point, making them excellent thermal barriers resistant to wear, erosion and corrosion. The combination of MSZ coatings and intermetallic self-bonding alloys Ni-Al results in coatings with excellent physical and mechanical properties, such as high hardness or resistance to oxidation and corrosion. This makes MSZ a suitable protective solution in various applications [6, 7]. Research into self-bonding Ni-Al alloys has been ongoing for the last decade and they are used in spray processes to provide protection against wear and corrosion, as well as for special applications such as thermal, electrical and biomedical purposes [8]. When the Ni-Al alloy is applied, an exothermic reaction occurs, resulting in partial fusion between the coating and the substrate, which significantly increases the bond strength [9]. This is the main reason for applying an Ni-Al alloy. The current paper presents the research results of reinforcing 10MgO-ZrO_2 (MSZ) with an Ni-Al reaction during flame spray coating to improve mechanical and structural properties, which are investigated in detail.

2. Experimental

2.1. Raw powders

The powders were supplied by Sulzer-Metco (US) Inc. The self-bonding material consisted in Amdry 995 with a nominal composition in wt% of Ni50-Al50. The ceramic powder of magnesia stabilised zirconia (MSZ) consisted of 10MgO-ZrO_2. The Ni-A1/MSZ raw composite powder of 45 µm, 99.6% purity was ball milled by a conventional tumbler ball mill incorporating a hardened steel jar and balls. The experiment was conducted at room temperature with a ball-to-powder ratio of 20 : 1 and a rotating speed of 75 rpm. Samples were collected after 1 h of milling, resulting in a particle size of approximately 60 nm. These samples were further investigated.

2.2. Substrate preparation

In this work, square-shaped coupons 26.5 × 26.5 mm with a thickness of 3.5 mm were used as the substrate. They were made of low carbon steel type API 5L, which is widely used in oil pipelines and the oil industry. Table 1 shows analysis of the substrate elements using a X-ray fluorescence (XRF) elemental analyser supplied by OXFORD (X-MET5000).

Table 1. Chemical composition of oil pipe substrate
Tabela 1. Skład chemiczny rury do transportu ropy naftowej

Element	C	Mn	P	S	Cu	Ni	Cr	Mo	V
Weight [%]	0.30	1.20	0.05	0.045	0.40	0.40	0.40	0.150	0.08

The substrate was cleaned by degreasing to remove any potential contaminants such as oil dust, rust and salts. In order to produce a rough surface for good adhesion, the low carbon steel substrates were blasted with aluminium oxide (Al_2O_3) with a particle size of ≈5 µm in a blasting cabinet at a pressure of 5 bar to improve adhesion between the thick coating and the substrate. The surface was first sandblasted to prepare it and then air-cleaned to remove any remaining dust particles. Finally, a roughness of 3–4 µm was achieved and the samples were ready for spray coating with Ni-Al/MSZ co-composites.

2.3. Flame spray coating

The flame spraying technique was carried out using a Swiss ROTOTEC 80 Castolin + Eutectic system. The optimal spray parameters used to obtain the thick top coatings are summarised in Table 2.

Table 2. Operating parameters for flame spray coating process of cermet Ni-Al/MSZ coating
Tabela 2. Parametry natryskiwania płomieniowego powłoki cermetalowej Ni-Al/MSZ

Parameters	Values
Spray nozzle diameter [mm]	6
Powder feed rate [g/min]	35–40
Spray distance [cm]	20
Pure fuels oxy-acetylene (O_2 + C_2H_2)	0.7–4
Coating thickness [mm]	1.85
Air pressure [MPa]	0.90
Heat treatment after thermal spraying (500, 750, 1000, 1100) [°C]	1000
Number of rotations	5
Temperature of flame spray [°C]	≈3000
Particle size of powder [nm]	60
Time between two sprays [s]	6

2.4. Cermet coating characterization

The above techniques were used to investigate the morphology and microstructure of both powder particles and as-sprayed coatings with different structures. Specifically, a scanning electron microscope (SEM) equipped with an energy dispersive X-ray (EDAX) analyser, model Jeol JIB-4610F, was used to examine the samples. The phase composition was analysed by X-ray diffraction (XRD) using a Philips diffractometer and filtered Cu$K\alpha$ radiation (λ = 0.154 nm), with the goniometer set at a scan rate of 0.05°/s over a 2Θ range from 20° to 70°. Finally, the microhardness of the polished surfaces of individual samples was measured using a Wilson 40 Vickers indenter (MVD) with a load of 250 g and a dwell time of 10 s. The microhardness of the surface coating (HV) was taken as the average of five tests. All surface points are approximately similar. Finally, the tensile bond strength was determined by the tensile pull method as an average of three measurements.

3. Results and discussion

3.1. Microstructure at various spray distances

Low carbon steel alloy type API 5L from the crude oil environment of the North Oil Company's Baiji field in Iraq have been used as samples. The results present themselves as follows.

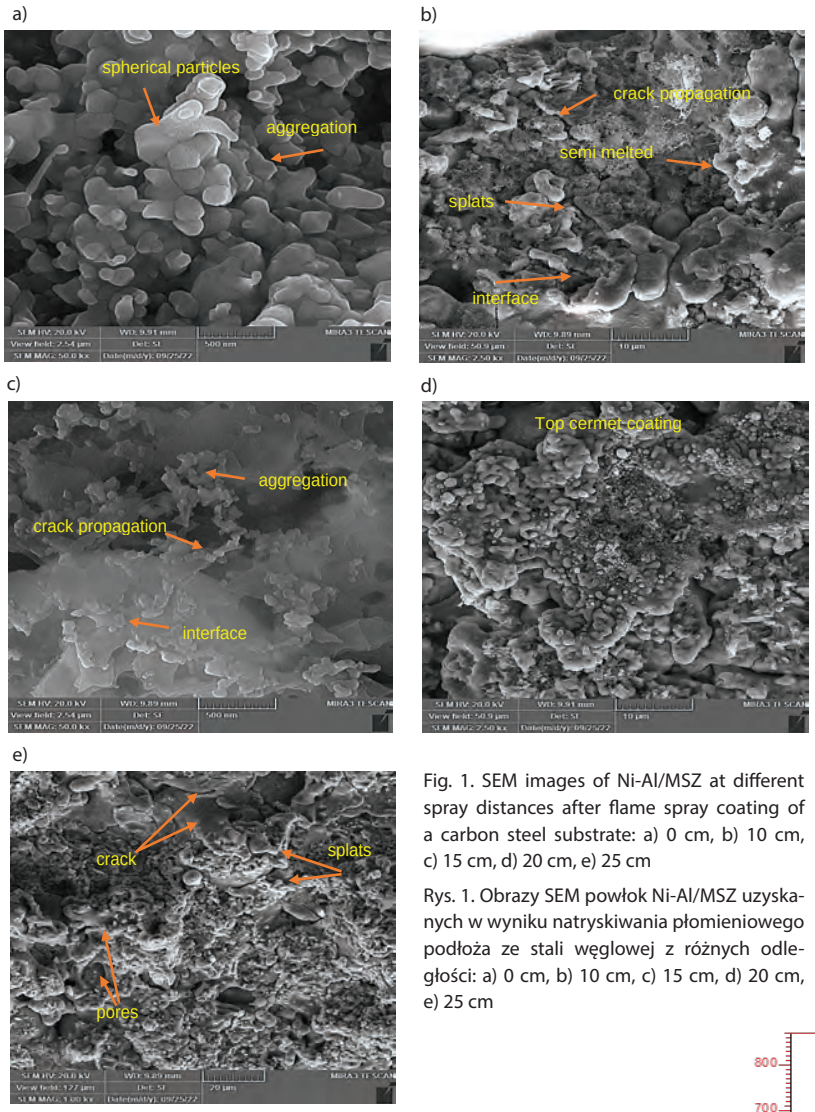

Fig. 1. SEM images of Ni-Al/MSZ at different spray distances after flame spray coating of a carbon steel substrate: a) 0 cm, b) 10 cm, c) 15 cm, d) 20 cm, e) 25 cm

Rys. 1. Obrazy SEM powłok Ni-Al/MSZ uzyskanych w wyniku natryskiwania płomieniowego podłoża ze stali węglowej z różnych odległości: a) 0 cm, b) 10 cm, c) 15 cm, d) 20 cm, e) 25 cm

The overall thickness of the Ni-A1/MSZ coating and coating features at various spray distances: 10 cm, 15 cm, 20 cm, 25 cm, obtained by SEM micrographs are shown in Fig. 1. Fig. 1a shows the initial Ni-Al/MSZ starting cermet powders used. It shows that all particles are spherical shapes of uniform size. This figure also shows the occurrence of large and homogenous ZrO_2, MgO particles, as well as Ni-Al particles, which are smaller. This is probably due to the longest mixing time (1 h), which produces the best homogenous microstructure. In Fig. 1b at a spray distance of 10 cm, we found a randomly weak and denser surface morphology. The top cermet coating shows a non-homogenous distribution with more frequent cracks and small pores. In fact, the shortest spray distance (10 cm) produces highly scattered and flattened particles as shown in Fig. 1b. This phenomenon indicates that the evaporation time of the droplets is too short and the particles are not completely melted [10].

Likewise, the SEM figure of the 15 cm spraying distance, shown in Fig. 1c, has a significant modifying role in grain formation, clearly indicating a dominant effect. It produces smooth spherically rounded particles which begin to form agglomerates throughout. With increasing spray distance to 20 cm, as shown in Fig. 1d, we observed a large rate of diffusion during this stage of the thermal spraying process. Worth noting also is the good adhesive force of the spherically shaped cluster aggregate particles [11]. A greater concentration of welded particles is visible, as shown by the increased number of agglomerated particles in Fig. 1d. At a further spray distance of 25 cm (Fig. 1e) individual splats can be clearly identified, which indicates a weak lamellar surface coating [12]. The structure of the deposited coating is reflective of the extent of particle melting that occurred at a significant distance prior to impacting the surface [13]. The top coating of cermet Ni-Al/MSZ also revealed different levels of pores along the interface between the coating surfaces, which proved to be dependent on the spraying distance [11, 13]. Publications on similar subjects also indicate that the evaporation time of particle droplets is not sufficient enough to melt the particles [14]. Additionally, we noticed that the cluster aggregate's spherically shaped particles are extremely rare, which could be connected to the long distance of the substrate, extending the time needed for the melted particles to reach the substrate [15]. Finally, it is concluded that the best spraying distance is 20 cm, as it provides a more uniform surface with a thickness of 1.85 mm and is sufficient to protect surface defects.

Fig. 2 shows the EDX spectra of the Ni-Al/MSZ as-sprayed top coatings showing elemental compositions at a spray distance of 20 cm – typical EDX spectra for all elemental Zr, Mg, O, Ni and Al peaks. The quantity of the powders is roughly identical to the elements

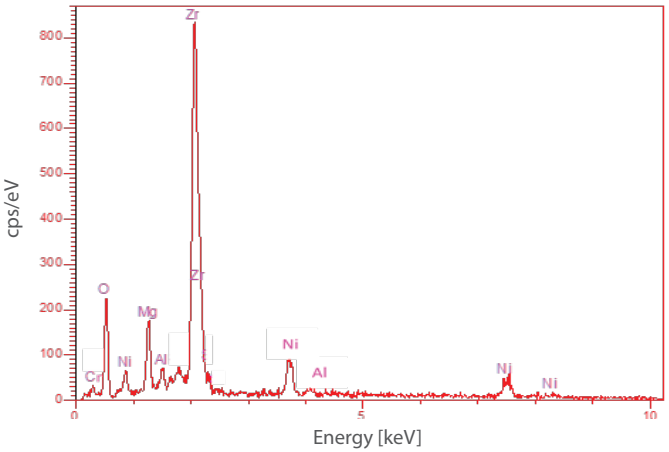

Element	Line	%wt
Cr	Ka	1.03
O	Ka	27.95
Mg	Ka	9.67
Al	Ka	4.96
Ni	Ka	5.18
Zr	La	51.21
		100.00

Fig. 2. Typical spectrum EDX of Ni-Al/MSZ coating obtained by flame spraying

Rys. 2. Typowe widmo EDX powłoki Ni-Al/MSZ uzyskanej metodą natryskiwania płomieniowego

in the ceramic coating. The EDX analysis also detected a large amount of O_2 related to the presence of NiO and Al_2O_3, which may be formed and grow within the ceramic ZrO_2-MgO during flame thermal spraying [16]. Traces of Cr were also detected; the presence of chrome, originating in the production process, caused an increase in the mechanical properties [17].

No other elemental contamination coming from the mixing media or from the flame spraying process was observed. The EDX results are identical and consistent with the XRD analysis, both of which clearly prove the absence of foreign elements.

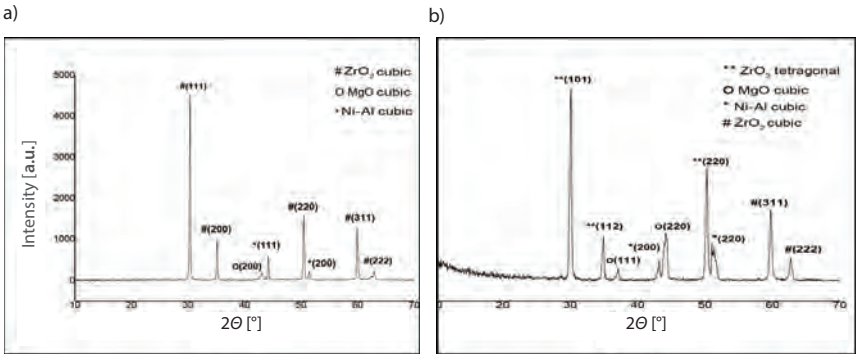

Fig. 3. XRD patterns of Ni-Al/MSZ as: a) powders, b) coating

Rys. 3. Wykresy XRD Ni-Al/MSZ dla: a) proszków, b) powłok

3.2. Phase composition analysis of Ni-Al/MSZ powders

This phase analysis was determined using XRD diffraction patterns before and after the application of top coatings, as presented in Fig. 3. In Fig. 3a, the powders exhibited diffraction peaks of 111, 200, 220, 311, and 222, which were attributed to the cubic phases of zirconia, Ni-Al, and MgO. Notably, the cubic zirconia phase had a much higher intensity compared to the MgO and Ni-Al phases. Additionally, the cubic MgO phase was observed to have a peak of 200 at $2\Theta = 43.065°$. The self-bonding Ni-Al cubic phase was also observed at $2\Theta = 44.225°$ and $2\Theta = 51.462°$ for 111 and 200 respectively. In addition, narrowing peaks for cubic peaks can be clearly observed. In Fig. 3b, after spraying, the Ni-Al/MSZ coating shows a changeable phase compared with the initial powders (Fig. 3a). Diffracted new peaks such as 101 and 112 are clearly detected at $2\Theta = 30.076°$ and $2\Theta = 34.923°$ respectively, which are characteristic of the tetragonal phase. It can be seen that overlaps occurred between $2\Theta = 43.168°$, $2\Theta = 44.222°$, also at $2\Theta = 50.262°$ and $2\Theta = 51.117°$. This splitting appeared clearly at high diffraction angle positions only. This phenomena signify that a transformation of phases from cubic to tetragonal occurred [18, 19]. No trace was found indicating the formation of a monoclinic phase, while the structures of MgO, Ni-Al, and ZrO_2 still dominated as a face-centered cubic (FCC), giving peaks of 111, 200, 220, and 311, 222 for ZrO_2.

3.3. Mechanical properties

3.3.1. Porosity of Ni-Al/MSZ cermet coating under heat treatment

The thick sprayed coating samples (1.85 mm) were subjected to several tests which included microhardness, porosity and adhesion force. The relationship between spray distance and other physical properties are discussed before and after sintering heat treatment. These parameters of the Ni-Al/MSZ cermet coating are explained in detail in the following points.

Fig. 4 illustrates the relationship between porosity and different spray distances: 10 cm, 15 cm, 20 cm and 25 cm. The results show that the lowest porosity of 7.016% was achieved at a spray distance of 20 cm, with porosity gradually decreasing as the distance increased [19, 20]. However, porosity started to increase again at distances greater than 25 cm, which is attributed to the failure of the molten material to distribute evenly out of the spray gun. Consequently, the flight time of the particles increased, resulting in semi-molten particles reaching the surface of the substrate. The aim of reducing porosity in the Ni-Al/MSZ coating composition led to the implementation of heat

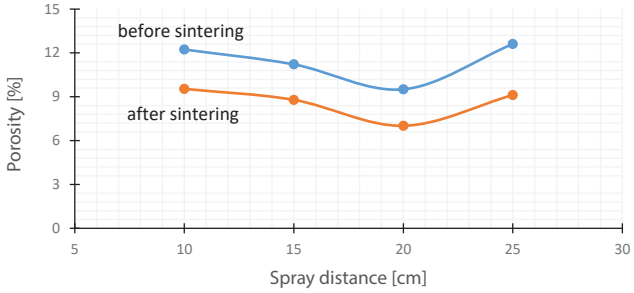

Fig. 4. Relationship between the spraying distance and porosity before and after heat treatment of cermet coating at a sintering temperature of 1000°C for 1 h

Rys. 4. Zależność między odległością natryskiwania a porowatością przed obróbką cieplną i po obróbce cieplnej powłoki cermetalowej w temperaturze spiekania 1000°C przez 1 h

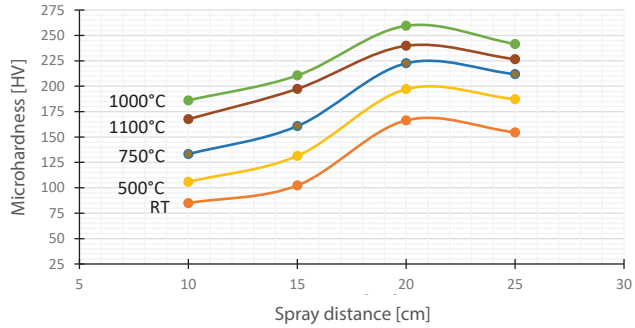

Fig. 5. Vickers microhardness of Ni-Al/MSZ coating sintered for 1 hour at various temperatures as a function of spraying distance

Rys. 5. Mikrotwardość Vickersa powłoki Ni-Al/MSZ spiekanej przez 1 h w różnych temperaturach w funkcji odległości natryskiwania

treatment at a temperature of 1000°C for 1 h of sintering. Before heat treatment, the highest porosity value was 9.512%, but after treatment decreased quickly to approximately 7.016% as shown in Fig. 4.

3.3.2. Effect of heat treatment on the microhardness of Ni-Al/MSZ cermet coating

Depending on the ideal spray parameters, a relationship was discovered to exist between microhardness and the spray distance before and after heat treatment (1000°C for 1 h) for standard samples as shown in Fig. 5.

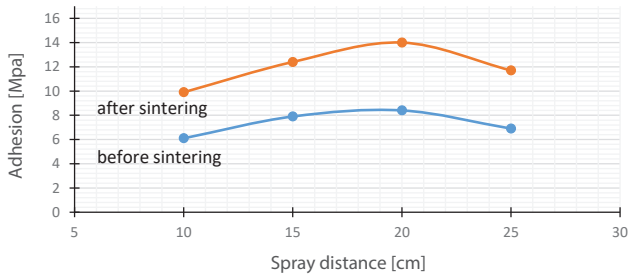

Fig. 6. Relationship between adhesion force and spray distance before and after heat treatment at 1000°C for 1 h

Rys. 6. Zależność między siłą adhezji a odległością natryskiwania przed obróbką cieplną i po obróbce cieplnej w temperaturze 1000°C przez 1 h

The microhardness values initially remain low as the distance between the spray gun and the base sample decreases. As the spray distance increases, the microhardness gradually increases and reaches its maximum value at a distance of 20 cm. Beyond that, the microhardness begins to decrease again. After subjecting the samples to a 1 h sintering heat treatment at 1000°C according to standard specifications, a significant increase in hardness values was observed at room temperature (166.4 HV) compared to 1000°C (259.5 HV), as shown in Fig. 5. This increase in hardness is attributed to the increased bonding between the atoms of the Ni-Al/MSZ coating layers, resulting from the elevated temperature during the heat treatment process. This also reduces the porosity of the cermet coating, contributing to the overall increase in hardness [20, 21].

3.3.3. Heat treatment impact on adhesion force of Ni-Al/MSZ cermet coating

The adhesion force of the Ni-Al/MSZ cermet coating was examined before and after the heat treatment process of 1 h at 1000°C, based on standard coating specifications. Prior to the heat treatment, the adhesion force was measured at 8.4 MPa, while after the treatment, it increased to 14 MPa. The adhesion force was also measured at different spray distances of 10 cm, 15 cm, 20 cm, and 25 cm, as shown in Fig. 6. The results indicate that adhesion force is initially low when the spray distance is small, then gradually increases with the increase of the spray distance until reaching the highest value at a distance of 20 cm. However, the adhesion force decreases suddenly when the spray distance exceeds 25 cm, possibly due to the formation of a weakened interface between the coating and the substrate. This phenomena is due to the unmelted particles at this distance which poorly bond with their surroundings causing porosity and microcracks in the cermet coating. These adhesion force results observed are identical with the results of microstructure, microhardness and porosity as shown in Fig. 1, Fig. 4 and Fig. 5 respectively. Finally, we may assert that, in the case of a spray distance of 20 cm, the particles typically melt in the flame stream completely to form molten droplets hitting the sample substrate, resulting in flat, thick layers [19, 21].

Also, the temperature of 1000°C significantly affected the self-bonding of Ni-Al on the coating, which had a considerable effect on the adhesion force results and possibly provided good wear resistance [21]. All the improvements originated from the unique spraying parameters chosen, which reduced the porosity of the layer and increased both the adhesion force and microhardness.

4. Conclusion

The following conclusions can be drawn from the work presented in this study:

- The authors sought to investigate the possibilities of using the flame spray coating method to protect a low carbon steel substrate type API 5L used in oil pipelines which often develop cracks and splits.
- The cermet coating consisting of a mix of self-bonding Ni-Al powders with ceramic 10MgO-ZrO_2 powders (60 nm) was successfully applied to inhibit defects in the pipe substrates.
- The coatings were made at four different spraying distances of 10 cm, 15 cm, 20 cm and 25 cm. The results showed that the best spray distance is 20 cm, which produces a small thick layer of 1.45 mm with a certain percentage of porosity: 9.512%.
- To determine the effect of the heat treatment on the hardness, porosity, thickness and adhesion force strength of a the thick cermet Ni-Al/MSZ coatings produced, the samples were subjected to heat treatment tests carried out at a rate of 5°C/min at 500°C, 750°C, 1000°C, 1100°C for 1 h of sintering, respectively. According to the results, the adhesion force and extremely weak porosity values improved after 1 h at 1000°C. The coating layers had a thickness of roughly 1.85 mm, which is suitable for protecting oil pipes. Also, the results showed that the cermet coating after treatment has significantly higher hardness (259.5 HV) compared to a low carbon steel (192.6 HV) substrate.
- The chemical composition of the cermet coating was determined by EDX analysis indicating that no contamination occurs during the spray coating. XRD results produced at RT identified only a single phase of FCC, but after sintering at 1000°C (for 1 h) clearly showed two phases, namely the face centered cubic (FCC) and tetragonal structure (T).
- Finally, the microstructure of the cermet coating was studied carefully by SEM, revealing a typical lamellar uniform structure, with particles agglomerated at 1000°C, while at a higher temperature (1100°C), a different irregular structure was found.

Acknowledgements

I particularly wish to acknowledge my supervisors Prof. Dr. Hamadi Khemakhem, and Prof. Dr. I. K. Jassim for providing me with important contributions and advice throughout my research. This work has been conducted at the university of Tikrit, Iraq at the physics and mechanical engineering departments cooperating with the North Oil Company in Baiji, and with the help of the Ministry of Science and Technology. I would like to thank the staff and skilled technical specialists for assistance in conducting the tests and the spray process.

CRediT authorship contribution statement

Mahmood M. Saleh: Conceptualization, Methodology, Project administration, Writing – review & editing.

Hamadi Khemakhem: Data curation, Software, Supervision, Validation, Writing – review & editing.

Ishmael K. Jassim: Formal analysis, Supervision, Writing – review & editing.

Raed Hashim Al-Saqa: Investigation, Resources, Visualization, Writing – original draft, Writing – review & editing.

BIBLIOGRAPHY

[1] R. Darolia. 2013. "Thermal Barrier Coatings Technology: Critical Review, Progress Update, Remaining Challenges and Prospects." *International Materials Review* 58(6): 315–348. DOI: 10.1179/1743280413Y.0000000019.

[2] B. D. Sartwell, P. E. Bretz. 1999. "HVOF Thermal Spray Coating Replaces Hard Chrome." *Advanced Materials and Processes* 156(2): 25–28.

[3] D. A. Stewart, P. H. Shipway, D. G. McCartney. 1999. "Abrasive Wear Behaviour of Conventional and Nanocomposite HVOF-Sprayed WC-Co Coatings." *Wear* 225–229(2): 789–798. DOI: 10.1016/S0043-1648(99)00032-0.

[4] R. H. Al-Saqa, I. K. Jassim, M. M. Uonis. 2023. "Effect of KCl on the Optical and Structural Properties of $CaZnO_3$ Perovskite Thin Films." *Ochrona przed Korozją* 66(8): 243–246. DOI: 1015199/40.2023.8.3.

[5] S. Mahade, C. Ruelle, N. Curry, J. Holmberg, S. Björklund, N. Markocsan, P. Nylén. 2019. "Understanding the Effect of Material Composition and Microstructural Design on the Erosion Behavior of Plasma Sprayed Thermal Barrier Coatings." *Applied Surface Science* 488: 170–184. DOI: 10.1016/j.apsusc.2019.05.245.

[6] M. Pytel, M. Góral, A. Nowotnik. 2016. "The Porosity Assessment of Ceramic Topcoat in Thermal Barrier Coatings Deposited by APS Method." *Advances in Manufacturing Science and Technology* 40(2): 53–65. DOI: 10.2478/amst-2016-0010.

[7] G. Chen, Y. Ling, Q. Li, H. Zheng, K. Li, Q. Jiang, L. Gao, M. Omran, J. Peng, J. Chen. 2020. "Stability Properties and Structural Characteristics of CaO-Partially Stabilized Zirconia Ceramics Synthesized from Fused ZrO_2 by Microwave Sintering." *Ceramics International* 46(10, Part B): 16842–16848. DOI: 10.1016/j.ceramint.2020.03.261.

[8] A. N. Khan, I. N. Qureshi. 2009. "Microstructural Evaluation of ZrO_2-MgO Coatings." *Journal of Materials Processing Technology* 209(1): 488–496. DOI: 10.1016/j.jmatprotec.2008.02.032.

[9] Q. Bai, C. Quyang, C. Zhao, B. Han, Y. Liu. 2021. "Microstructure and Wear Resistance of Laser Cladding of Fe-Based Alloy Coatings in Different Areas of Cladding Layer." *Materials* 14(11): 2839. DOI: 10.3390/ma14112839.

[10] L. Keerthana, C. Sakthivel, I. Prabha. 2019. "MgO-ZrO_2 Mixed Nanocomposites: Fabrication Methods and Applications." *Materials Today Sustainability* 3–4: 100007. DOI: 10.1016/j.mtsust.2019.100007.

[11] P. Carpio, A. Borrell, M. D. Salvador, A. Gómez, E. Martínez, E. Sánchez. 2015. "Microstructure and Mechanical Properties of Plasma Spraying Coatings from YSZ Feedstocks Comprising Nano- and Submicron-Sized Particles." Ceramics International 41(3, Part A): 4108–4117. DOI: 10.1016/j.ceramint.2014.11.106.

[12] E. Sánchez, E. Bannier, M. D. Salvador, V. Bonache, J. C. García, J. Morgiel, J. Grzonka. 2010. "Microstructure and Wear Behavior of Conventional and Nanostructured Plasma-Sprayed WC-Co Coatings." *Journal of Thermal Spray Technology* 19: 964–974. DOI: 10.1007/s11666-010-9480-5.

[13] R. B. Wijayanti, I. Rosmayanti, K. Wahyudi, E. Maryani, H. Hernawan, R. Septawendar. 2021. "Preparation of Magnesia Partially Stabilized Zirconia Nanomaterials from Zirconium Hydroxide and Magnesium Carbonate Precursors Using PEG as a Template." *Crystals* 11(6): 635. DOI: 10.3390/cryst11060635.

[14] J. H. Yan, J. J. Xu, Rafi-ud-din, Y. Wang, L. F. Liu. 2015. "Preparation of Agglomerated Powders for Air Plasma Spraying $MoSi_2$ Coating." *Ceramics International* 41(9, Part A): 10547–10556. DOI: 10.1016/j.ceramint.2015.04.149.

[15] R. H. Al-Saqa, I. K. Jassim. 2023. "Effect of Substrate Temperature on the Optical and Structural Properties of $CaZnO_3$ Perovskite Thin Films." *Digest Journal of Nanomaterials and Biostructures* 18(1): 165–172. DOI: 10.15251/DJNB.2023.181.165.

[16] H. Juliano, F. Gapsari, H. Izzuddin, T. Sudiro, K. Y. Phatama, W. P. Sukmajaya, Zuliantoni, T. M. Putri, A. M. Sulaiman. 2022. "HA/ZrO_2 Coating on CoCr Alloy Using Flame Thermal Spray." *Evergreen Joint Journal of Novel Carbon Resource Sciences and Green Asia Strategy* 9(2): 254–261.

[17] A. Baadi. 2020. *Laser Remelting of Yttria Stabilized Zirconia Coatings Deposited by Suspension Plasma Spraying*. Master thesis. Montréal, Québec, Canada: Concordia University.

[18] L. Thair, I. K. Jassim, S. R. Al- Khuzaie, J. F. Hammody, M. H. Kalil. 2016. "Corrosion Protection of Carbon Steel Oil Pipelines by Unsaturated Polyester/Clay Composite Coating." *American Scientific Research Journal for Engineering, Technology, and Sciences* 18(1): 108–119.

[19] Z. Li, Y. Zhao, G. Liu, C. Cao, Q. Liu, D. Zhao, X. Zhang, C. Zhao, H. Yu. 2022. "Parametric Studies on Finishing of AZ31B Magnesium Alloy with Al_2O_3 Magnetic Abrasives Prepared by Combining Plasma Molten Metal Powder with Sprayed Abrasive Powder." *Micromachines* 13(9): 1369. DOI: 10.3390/mi13091369.

[20] S. Y. Darweesh, I. K. Jassim, A. S. H. Mahmood. 2019. "Characterization of Cermet Composite Coating Al_2O_3-Ni System." *Journal of Physics: Conference Series* 1294(2): 022011. DOI: 10.1088/1742-6596/1294/2/022011.

[21] I. K. Jassim, M. A. Abdullah. 2020. "Characteristics Structural and Physical Properties of the System Cermet [Basalt-(Ni-Al)] Using Thermal Spray Flame Technology." *NeuroQuantology* 18(4): 37–44. DOI: 10.14704/nq.2020.18.4.NQ20159.